Nuclear quadrupole interaction studies of $C15$ $R\mathrm{Mn}_2$ hydrides (R=Y,Gd,Tb,Dy)

M. Forker,[1,*] S. C. Bedi,[1,†] and H. Euler[2]
[1]*Helmholtz Institut für Strahlen-und Kernphysik, University of Bonn, Nussallee 14-16, D-53115 Bonn, Germany*
[2]*Steinmann-Institut für Geologie, Mineralogie und Paläontologie, University of Bonn, Poppelsdorfer Schloss, D-53115 Bonn, Germany*
(Received 20 May 2008; published 8 September 2008)

The nuclear electric quadrupole interaction (QI) of the probe nucleus $^{111}\mathrm{In}/^{111}\mathrm{Cd}$ in the paramagnetic phase of the $C15$ rare earth (R)–manganese hydrides (deuterides) $R\mathrm{Mn}_2\mathrm{H}(D)_x$, with R=Y, Gd, Tb, and Dy, has been investigated by perturbed angular-correlation spectroscopy. The QI between the $^{111}\mathrm{Cd}$ quadrupole moment and the electric-field gradient (EFG) at the probe nucleus on the Mn site has been measured as a function of temperature in $\mathrm{TbMn}_2\mathrm{H}(D)_x$ in the concentration range $0 \leq x \leq 4.3$ and in $R\mathrm{Mn}_2\mathrm{H}(D)_x$, R=Y,Gd,Dy at the highest H content of $x \sim 4.3$. The relative temperature dependence of the EFG in the parent compounds $R\mathrm{Mn}_2$ is twice as strong as in isostructural $R\mathrm{Al}_2$ which can be related to differences in the Debye temperatures resulting from different radius ratios r_R/r_{Mn} and r_R/r_{Al} [Joseph-Gschneidner postulate, Scr. Metall. **2**, 631 (1968)]. Hydrogenation of $R\mathrm{Mn}_2$ increases the magnitude of the EFG by a factor of 2 between x=0 and x =4.3 but leaves the relative temperature dependence almost unchanged. Only at concentrations $x > 3.6$ the temperature coefficient of the QI is significantly larger than in uncharged $R\mathrm{Mn}_2$. These results are compared with the much stronger concentration dependence and the anomalous temperature dependence of the QI of $^{111}\mathrm{Cd}$ in the $C15$ hydrides $\mathrm{HfV}_2\mathrm{H}_x$. Evidence for an exceptionally high H mobility in $\mathrm{TbMn}_2\mathrm{H}_x$ is presented. The measurements provide information on structural changes and magnetic ordering temperatures at different H concentrations.

DOI: 10.1103/PhysRevB.78.104202 PACS number(s): 76.80.+y, 71.70.Jp, 74.70.Ad, 81.05.Je

I. INTRODUCTION

$R\mathrm{Mn}_2$ (R=rare earth) are among the Laves phase compounds which may absorb large quantities of hydrogen. The influence of the H concentration on the structure and on the complex magnetic properties of these intermetallics has attracted interest for many years. A review of the present understanding based on x-ray and neutron diffractions, magnetometry, and hyperfine interaction (HFI) techniques such as NMR, μSR, and Mössbauer spectroscopy has recently been given by Paul-Boncour.[1]

For R=Sm, Gd, Tb, Dy, and Y the $R\mathrm{Mn}_2$ Laves phases crystallize in the cubic $C15$ structure.[2] The Mn site ($16d$) of the $C15$ structure has axial point symmetry so that nuclei on this site are subject to an axially symmetric electric-field gradient (EFG) which can be determined by measuring its interaction with the quadrupole moment of a probe nucleus. Measurements of nuclear quadrupole interactions (QIs) in $C15$ $R\mathrm{Mn}_2$ compounds have been reported for YMn_2,[3] $\mathrm{Y}_{0.96}\mathrm{Sc}_{0.04}\mathrm{Mn}_2$,[4] GdMn_2, and TbMn_2.[5] The QI in $C14$ YMn_2, synthesized under high pressure, has been investigated by Komissarova *et al.*[6] These studies were carried out with the perturbed angular-correlation (PAC) technique using the radioisotope $^{111}\mathrm{In}/^{111}\mathrm{Cd}$ as probe nucleus.

In contrast to the wealth of information on the influence of the H concentration on the magnetic properties and magnetic hyperfine interactions, little is known about the effect of the H load on the QI in $R\mathrm{Mn}_2$ hydrides. Up to now the effect of hydrogenation on the static and dynamic QIs in $C15$ hydrides has been investigated only for the V compounds $M\mathrm{V}_2\mathrm{H}_x$, M=Ta, Zr, and Hf, using $^{51}\mathrm{V}$ NMR (Refs. 7–9) and $^{111}\mathrm{Cd}$ PAC spectroscopy.[10]

The most interesting results of these studies—besides valuable information on H(D) diffusion and phase transitions—concern the concentration and temperature dependence of the static quadrupole frequency ν_q. In $\mathrm{ZrV}_2\mathrm{H}_x$ and $\mathrm{HfV}_2\mathrm{H}_x$ an increase in the H load x was found to produce a strong increase in the room-temperature (RT) EFG with the same relative magnitude for $^{51}\mathrm{V}$ and $^{111}\mathrm{Cd}$. The investigation of the temperature dependence of the EFG in $\mathrm{HfV}_2\mathrm{H}_x$ by $^{111}\mathrm{Cd}$ PAC leads to particularly intriguing results: in the parent compound HfV_2 and at small x of $\mathrm{HfV}_2\mathrm{H}_x$ the $^{111}\mathrm{Cd}$ QI frequency ν_q increases with increasing temperature—a highly unusual observation for a metallic system. However, the normal trend of a negative temperature coefficient $\alpha \equiv \delta \ln \nu_q / \delta T < 0$ can be restored by rising the H load to $x > 1.5$.

It has been proposed[10] that these observations might be related to the particular band structure of HfV_2 where the Fermi energy falls into a sharp peak of the density-of-states (DOS) curve[11] and hydrogenation leads to a pronounced decrease in $N(E_F)$.[12] More data on the concentration and temperature dependence of the EFG in $C15$ hydrides, preferably with the same probe nucleus, could help us to corroborate this interpretation and thus advance the understanding of electric-field gradients in metallic systems and in particular their temperature dependence.

In this context, the rare earth–manganese hydrides $R\mathrm{Mn}_2\mathrm{H}_x$ are attractive candidates for further studies. At temperatures $T \geq 350$ K $R\mathrm{Mn}_2\mathrm{H}_x$ with R=Y, Gd, Tb, and Dy maintain the cubic $C15$ structure of $R\mathrm{Mn}_2$ up to the highest H content of $x \sim 4.3$; they thus have the same structure as $\mathrm{HfV}_2\mathrm{H}_x$, similar lattice parameter and the H atoms mainly occupy the same interstitial g sites, but differently from $\mathrm{HfV}_2\mathrm{H}_x$ hydrogenation of $\mathrm{Y}(R)\mathrm{Mn}_2$ shifts the position of the Fermi energy from a valley in the DOS curve to slightly higher $N(E_F)$ values.[13] H(D) diffusion in $R\mathrm{Mn}_2\mathrm{H}_x$ and information on magnetic and structural properties are further as-

pects motivating the investigation of these hydrides. In this paper we report a PAC study of static and dynamic QIs of ^{111}Cd in the parent compounds RMn_2, R=Y, Gd, Tb, and Dy, in the hydrides $TbMn_2H(D)_x$ in the concentration range $0 \leq x \leq 4.3$ and in RMn_2H_x, R=Y, Gd, and Dy at the highest concentration of $x \sim 4.3$ as a function of temperature.

II. EXPERIMENTAL DETAILS

A. Sample preparation and equipment

The 171–245 keV PAC cascade of ^{111}Cd is populated by the electron-capture decay of the 2.8d isotope ^{111}In. The intermediate state of the cascade has a half-life of $T_{1/2}$=84 ns and its spin is I=5/2. Samples of RMn_2, R=Y, Gd, Tb, and Dy synthesized by arc melting of the metallic constituents in argon atmosphere, were doped with ^{111}Cd by diffusion in vacuum (800 °C, 12–24 h) of carrier-free radioactive ^{111}In (concentration $\leq$1 ppm) into the host lattice.

Radioactive hydrides $RMn_2H(D)_x$, R=Y, Gd, Tb, and Dy, were produced by first outgassing the doped parent compounds RMn_2 at 1300 K for 1–2 h in a quartz tube connected to a vacuum of 10^{-7} mbar. A known quantity of $H(D)_2$ gas with a purity of 99.9999 at. % was then admitted into the calibrated volume at $T \sim 295$ K. Absorption usually sets in after a few minutes of exposure. The absorbed quantity of hydrogen was determined from the pressure decrease in the calibrated volume. By variation of the initial hydrogen pressure between 100 and 900 mbar hydrides $RMn_2H(D)_x$ with different $H(D)$ concentrations of $x \leq 4.3$ could be obtained. Among the RMn_2H_x hydrides, $TbMn_2H_x$ was studied in most detail. For this compound the HFI was investigated as a function of temperature at hydrogen concentrations $0.4 \leq x \leq 4.3$. The increase in the $C15$ lattice parameter a with increasing H load of $TbMn_2H_x$, determined by room-temperature x-ray diffraction, was in agreement with the result of Figiel *et al.*[14] We also searched for possible isotope effects on the HFI parameters, in particular on the spin-relaxation constant,[15] by extending the measurements to the deuterides RMn_2D_x with concentrations x=1.2, 2.56, and 4.15. For the constituents R=Y, Gd, and Dy the measurements were limited to the parent compounds RMn_2 and to the hydride with the maximum hydrogen concentration $x \sim 4.3$.

The PAC measurements were carried out with a standard four-detector BaF_2 setup in the temperature range 15 K $\leq T \leq$ 600 K. Temperatures $T <$ 290 K were obtained with a closed-cycle He refrigerator; temperatures $T >$ 290 K were produced with a especially designed PAC furnace.[16] For measurements at $T >$ 290 K, the samples were encapsulated under vacuum into small quartz tubes.

B. Data analysis

The modulation in time of a γ-γ angular correlation by a static HFI can be described by the perturbation factor,[17]

$$G_{kk}(t;\nu_q,\eta,\delta) = s_{k0} + \sum_n s_{kn}\cos(\omega_n t)\exp(-1/2\,\delta\omega_n t). \tag{1}$$

The hyperfine frequencies ω_n are related to the energy differences of the hyperfine levels into which the nuclear state is split by the HFI. In the most general case, these frequencies and the amplitudes s_{kn} have to be determined by diagonalization of the interaction Hamiltonian. The number n of terms in Eq. (1) depends on the spin of the nuclear state and the multipole order of the interaction. The exponential factor accounts for possible distributions of the static HFI caused by structural or chemical defects, which lead to an attenuation of the oscillatory PAC pattern. The parameter δ is the relative width of a Lorentzian distribution.

In the case of a static QI, the frequencies ω_n depend on the quadrupole frequency $\nu_q = eQV_{zz}/h$ and the asymmetry parameter $\eta = (V_{xx} - V_{yy})/V_{zz}$, where $V_{ii} = \delta^2 V/\delta i^2$ $(i = x, y, z)$ are the principal-axes components of the EFG tensor with $|V_{xx}| \leq |V_{yy}| \leq |V_{zz}|$. In polycrystalline samples the amplitudes s_{kn} are functions of η only. In the magnetically ordered phase of RMn_2H_x, a static magnetic hyperfine field B_{hf} is expected to act on the probe nuclei in addition to the QI. In this case the hyperfine frequencies ω_n depend on five parameters: the magnetic frequency $\nu_m = g\mu_N B_{hf}/h$ (g denotes the nuclear g factor), the QI parameters ν_q and η, and the Euler angles β and γ which describe the relative orientation of the magnetic hyperfine field and the EFG tensor.

The motion of the H atoms in a hydride is known to cause a time dependence of the QI which leads to nuclear relaxation. The effect of such H jumps on the angular correlation is most appropriately described by Blume's stochastic theory.[18,19] Frequently, an approximation of the Blume theory[18] with a single relaxation parameter λ_k is used in the data analysis,

$$G_{kk}(t) = \Gamma_{kk}(t)\exp(-\lambda_k t). \tag{2}$$

The validity of this approximation, the form of the function $\Gamma_{kk}(t)$, and the relation between the relaxation parameter λ_K and the jump rate w are discussed in Refs. 20 and 21. When several fractions of nuclei subject to different HFIs are found in the same sample, the effective perturbation factor is given by

$$G_{kk}(t) = \Sigma_i f_i G^i_{kk}(t), \tag{3}$$

where f_i (with $\Sigma_i f_i = 1$) is the relative intensity of the ith fraction. For sites with vanishing HFI the angular correlation is unperturbed and one has $G_{kk}(t) = 1$.

III. MEASUREMENTS AND RESULTS

Figures 1 and 2 illustrate the typical ^{111}Cd PAC spectra observed in $C15$ RMn_2 parent compounds and RMn_2H_x hydrides using $TbMn_2$ and $TbMn_2H_{0.8}$ as examples. For comparison (see Sec. IV C) we also show in Fig. 3 some PAC spectra from our previous study[10] of ^{111}Cd in the $C15$ hydride $HfV_2H_{1.78}$.

Hydrogenation leads to changes in the HFI parameters but has little effect on the structure of the PAC spectra of RMn_2H_x. Starting at high temperatures, one first finds—both in unloaded RMn_2 and loaded RMn_2H_x—a periodic QI modulation of the anisotropy with time which is characteristic for a static axially symmetric QI. As the magnetically ordered phase is approached, the amplitude of the periodic modulation decreases and finally gives way to strongly at-

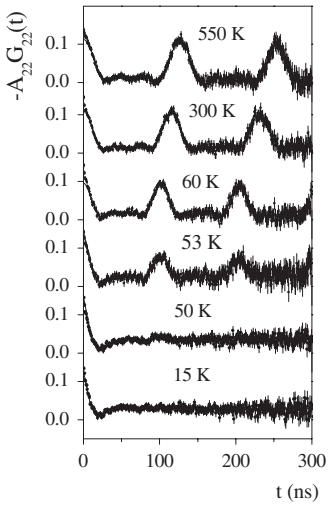

FIG. 1. PAC spectra of ^{111}Cd in $TbMn_2$ at different temperatures.

tenuated PAC spectra. As this attenuation is correlated with magnetic order, it is likely to be caused by a distribution of the magnetic hyperfine field, possibly reflecting instability of the Mn moment. Close to the ordering temperature T_N the spectra consist of a superposition of the distributed magnetic and periodic QI component. The analysis in terms of a two-component model allows the determination of T_N and of the temperature dependence of the paramagnetic fraction. In the following we present the results of the data analysis for RMn_2 and RMn_2H_x, respectively.

A. ^{111}Cd in *C*15 RMn_2 Laves phases (R=Y,Gd,Tb,Dy)

The quadrupole frequency ν_q of ^{111}Cd on the Mn site (16*d*) of RMn_2 was extracted by fitting Eq. (1) to the measured spectra. In all cases the asymmetry parameter was

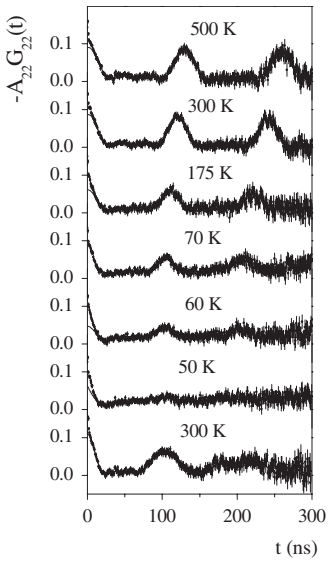

FIG. 2. PAC spectra of ^{111}Cd in $TbMn_2H_{0.8}$ at different temperatures. The bottommost spectrum corresponds to $TbMn_2H_{0.8}$ at 300 K taken after hydrogenation prior to any heat treatment.

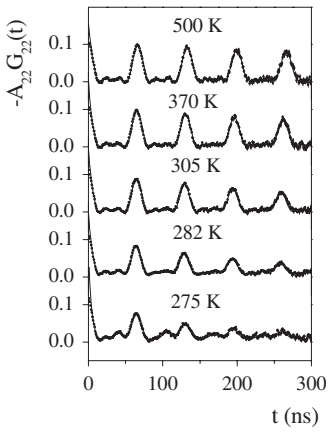

FIG. 3. PAC spectra of ^{111}Cd in $HfV_2H_{1.78}$ in the temperature range 278 K$\leq T\leq$500 K taken from Ref. 10.

$\eta\leq 0.05$ and the width of the Lorentzian frequency distribution was $\delta\leq 0.03$. Our results for ^{111}Cd:$TbMn_2$ agree with the previous measurements of Tulapurkar and Mishra;[5] in the case of ^{111}Cd:$GdMn_2$ our values are ~7% larger than those of Ref. 5. The quadrupole frequencies for R=Y, Gd, Tb, and Dy are collected in Fig. 4 which also illustrates the anomalous temperature dependence of the QI of ^{111}Cd in HfV_2 (Ref. 10) and—for comparison with $GdMn_2$—that of $GdAl_2$.[23] The ν_q values of YMn_2 at $T<295$ K in Fig. 4 have been determined by Tulapurkar *et al.*[3]

Close to T_N=50 K, a superposition of two components—one representing the magnetic phase with a distribution of the magnetic hyperfine field and the other one representing the paramagnetic phase with a well-defined QI—was fitted to the measured spectra. The resulting temperature dependence of the paramagnetic fraction f_p is shown in Fig. 5.

In the case of the strongly attenuated spectra at $T<T_N$, a precise determination of the parameters of the combined interaction is difficult. The best fit (solid line in the 15 K spectrum of Fig. 1) was obtained—with the QI parameters fixed

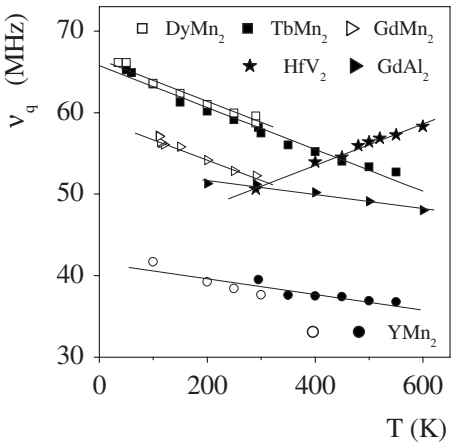

FIG. 4. The temperature dependence of the quadrupole frequency ν_q of ^{111}Cd in *C*15 Laves phases. The present results for RMn_2, R=Y, Gd, Dy, and Tb, are compared to $\nu_q(T)$ of ^{111}Cd in HfV_2 (full stars, Ref. 10) and $GdAl_2$ (full triangles, Ref. 23). The ν_q values of YMn_2 at $T\leq 300$ K (open circles) have been taken from Ref. 3.

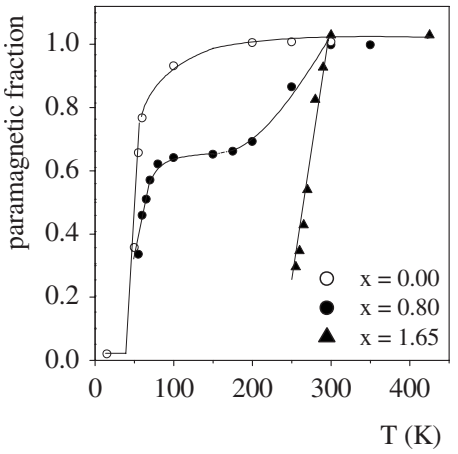

FIG. 5. The paramagnetic fraction of $TbMn_2$ and $TbMn_2H_x$, $x=0.80$ and 1.65, as a function of temperature. The solid lines are guides for the eye.

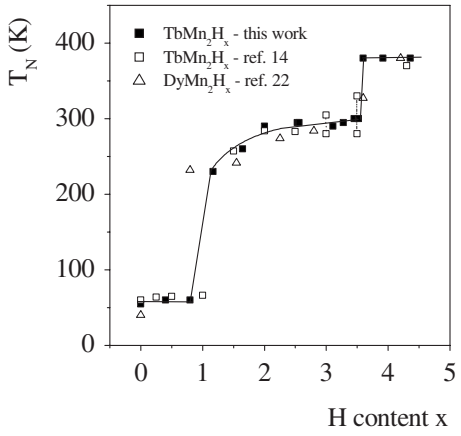

FIG. 6. The magnetic ordering temperature of $TbMn_2H_x$ (this work and Ref. 14) and $DyMn_2H_x$ (Ref. 22) as a function of the hydrogen content.

to their values in the paramagnetic phase—with a Lorentzian distribution ($\delta \sim 0.7$) of the magnetic interaction parameters centered at $\nu_m \sim 16$ MHz (corresponding to $B_{hf} \sim 7$ T), $\beta \sim 50°$.

The broad distribution of the magnetic hyperfine field was observed in all RMn_2 investigated here and in YMn_2 for which Tulapurkar and Mishra[5] found an oscillatory PAC pattern corresponding to a well-defined $B_{hf} \sim 11.5$ T. Distributions of the magnetic hyperfine field have also been reported for, e.g., ^{111}Cd in $Y_{0.97}Sc_{0.03}Mn_2$ (Ref. 4) and ^{57}Fe in $DyMn_2$.[22]

B. ^{111}Cd in $RMn_2H(D)_x$ (R=Y,Gd,Tb,Dy and $0.4 \leq x \leq 4.3$)

The bottommost spectrum in Fig. 2, taken after hydrogenation prior to any temperature treatment, shows a considerable line broadening reflecting an inhomogeneous hydrogen distribution. All hydride samples, encapsulated in quartz tubes, were therefore homogenized by heating to 550 K before starting the measurements of the QI. Annealing at $T > 550$ K led to an irreversible destruction of the oscillatory PAC pattern, probably caused by hydrogen induced amorphization. The same irreversible destruction was observed when the hydrogen was desorbed by heating the hydrides in vacuum to $T > 450$ K.

Two aspects are noteworthy in the PAC spectra of RMn_2H_x. (i) At H concentrations $x < 1.5$, the increase in the paramagnetic fraction f_p with temperature—mirrored by the amplitude of the periodic modulation of the anisotropy—occurs in two steps. As illustrated by Figs. 2 and 5 for $x=0.8$, a first increase to $f_p \sim 0.5$ between 55 and 80 K is followed by a plateau extending to $T \sim 200$ K and an increase to $f_p \sim 1$ from 200 to 300 K. At all concentrations $x > 1.5$, however, f_p grows continuously with increasing temperature [see as an example $f_p(T)$ of $x=1.65$ in Fig. 5] to reach saturation within a temperature interval of ~30–40 K. (ii) The second interesting aspect in the PAC spectra of $TbMn_2H_x$ is the absence of spin-relaxation effects which becomes evident by comparing the PAC spectra of $TbMn_2H_x$ to those of $HfV_2H_{1.78}$ (see Fig. 3). As temperature is lowered from 500 K, the spin precessions of $HfV_2H_{1.78}$ suffer an exponential attenuation which increases with decreasing temperature. This attenuation reflects the nuclear-spin relaxation induced by the fluctuations of the QI caused by jumping H atoms. Remarkably, at comparable temperatures and H content the amplitudes of the spin precessions in $TbMn_2H_x$ remain constant in time (see Fig. 2 for $x=0.8$). At none of the H or D concentrations investigated the PAC spectra showed an exponential loss of modulation amplitude. The maximum nuclear-spin-relaxation parameter λ_2^{max} [see Eq. (2)] compatible with the spectra of $TbMn_2H(D)_x$ ($0.4 \leq x \leq 4.3$) is $\lambda_2^{max} \leq 0.5$ MHz. In HfV_2H_x one has $\lambda_2^{max} \leq 10$ MHz.

Because of the absence of spin-relaxation effects, the PAC spectra were analyzed using Eqs. (1) and (3). The results of the analysis are collected in Figs. 5–8. Figure 5 shows the temperature dependence of the paramagnetic fraction for $x=0.0, 0.8, 1.65$, Fig. 6 the magnetic ordering temperature T_N as a function of the H content, Fig. 7 the x and T dependence of the quadrupole frequency ν_q, and Fig. 8 compares the concentration dependence of the quadrupole frequency of $TbMn_2H_x$ (at 400 K) to that of HfV_2H_x (at 300 K). Both $T_N(x)$ and $\nu_q(x;T)$ observed in RMn_2H_x remain unchanged when hydrogen is replaced by deuterium.

IV. DISCUSSION

A. Quadrupole interaction of ^{111}Cd in the $C15$ Laves phases RMn_2, RAl_2, and HfV_2

The quadrupole frequencies ν_q of ^{111}Cd in the parent compounds RMn_2, R=Y, Gd, Tb, and Dy, are displayed in Fig. 4 together with the results of previous studies of the $C15$ Laves phases HfV_2 (Ref. 10) and $GdAl_2$.[23] The RT value of ν_q in RMn_2 increases slightly from R=Gd to Dy. This trend which has also been observed for ^{111}Cd in RAl_2 (Ref. 23) is probably a consequence of the lanthanide contraction.

From Fig. 4 we note that only HfV_2 presents an anomaly in the temperature dependence of the ^{111}Cd QI. The positive temperature coefficient $\alpha \equiv \delta \ln \nu_q / \delta T > 0$ found in HfV_2 is thought to result from a thermal repopulation of Fermi-surface electrons. In Ref. 10 it has been shown that such

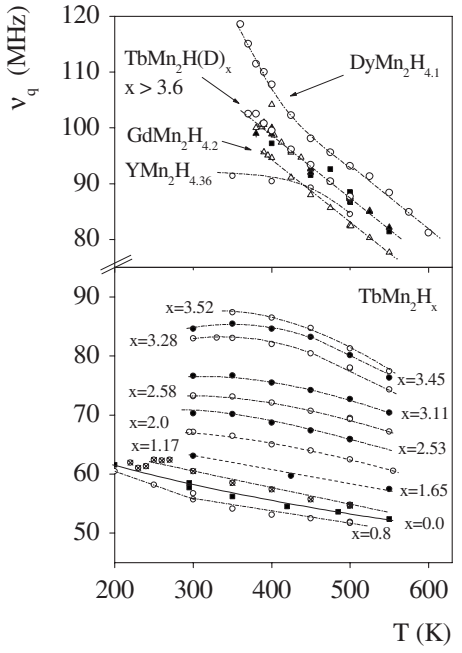

FIG. 7. The temperature dependence of the quadrupole frequency ν_q of ^{111}Cd in $TbMn_2H_x$ at different H contents (lower section) and in $RMnH_x$, R=Y, Gd, Tb, and Dy with $x \sim 4$.

effects can be expected preferentially in regions of large rapidly varying DOS which is the case of HfV_2.

In all other $C15$ Laves phases investigated up to now the quadrupole frequency shows the usual decrease with increasing temperature. The slope of the linear function is practically the same for all R constituents of a given RX_2 series but changes significantly with the X constituent: $\alpha \equiv \delta \ln \nu_q / \delta T \sim -4.0(2) \times 10^{-4}$ and $\sim -2.2(2) \times 10^{-4}$ K^{-1} for RMn_2 and RAl_2,[23] respectively. Furthermore, the temperature dependence in YMn_2 is weaker [$\alpha(YMn_2) \sim -2.0(4) \times 10^{-4}$ K] than in RMn_2, $R \neq Y$ (see Fig. 4), in contrast to the corresponding Al compounds where $\alpha(RAl_2) \approx \alpha(YAl_2)$.[23]

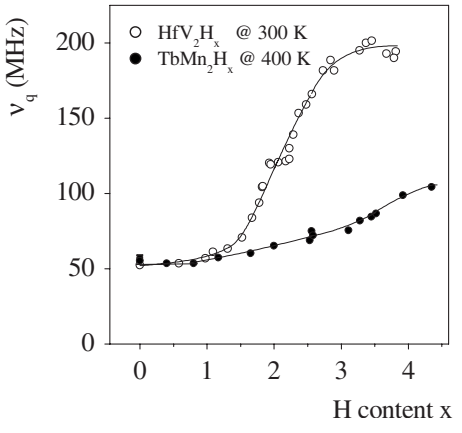

FIG. 8. The dependence of the quadrupole frequency of ^{111}Cd in $TbMnH_x$ at 400 K and in HfV_2H_x at 300 K (Ref. 10), respectively, on the hydrogen content x.

The temperature dependence of the EFG is governed by the phonon properties of the compound.[24] In many sp metals the temperature coefficient of the EFG was found[25] to be proportional to the quantity $(M\Theta_D^2)^{-1}$ (M—mass of the host atoms; Θ_D—Debye temperature), which is a measure of the mean-square vibrational amplitude of the host atoms. If we assume that the proportionality $\alpha \propto 1/(M\Theta_D^2)$ also holds for intermetallic compounds, the observation $\alpha(RMn_2) > \alpha(RAl_2)$ implies that the Debye temperature of RAl_2 is substantially larger than that of RMn_2. It is interesting to compare this conclusion with the Joseph-Gschneidner postulate[2,26] which relates the Debye temperature Θ_D of AB_2 Laves phases to the radius ratio r_A/r_B (with $r_A = \sqrt{3}a/8$; a=lattice parameter). The comparison of Θ_D and r_A/r_B for a number of Laves phases has shown that for $r_A/r_B > 1.225$ (ideal value for closest packing) the Debye temperature of AB_2 is closer to that of the A metal and for $r_A/r_B < 1.225$ closer to that of the B metal. In the present case, one has $r_A/r_B = 1.18$ and 1.27 for RAl_2 and $R(Y)Mn_2$, respectively, using $r_{Al} = 143$ pm and $r_{Mn} = 131$ pm from Ref. 27. Accordingly, the Debye temperature of RAl_2 should be closer to that of Al [$\Theta_D(Al) = 423$ K], the Debye temperature of RMn_2 closer to that of the R metals [$\Theta_D(R) \sim 180$ K (Ref. 28)], and that of YMn_2 closer to $\Theta_D(Y) = 258$ K. With $\alpha \propto 1/(M\Theta_D^2)$ the Joseph-Gschneidner[26] postulate thus predicts $\alpha(RMn_2) > \alpha(RAl_2)$ for $R \neq Y$, $\alpha(RMn_2) > \alpha(YMn_2)$, and $\alpha(RAl_2) \approx \alpha(YAl_2)$, which is in agreement with the experimental observations of the present work and of Ref. 23.

B. Concentration and temperature dependence of the quadrupole interaction of ^{111}Cd in RMn_2H_x

In Fig. 8 we compare the concentration dependence of the ^{111}Cd QI in $TbMn_2H_x$ (at 400 K) and HfV_2H_x (at 300 K). In both compounds the quadrupole frequency ν_q increases continuously with increasing H load, but for HfV_2H_x the increase $\delta \ln \nu_q / \delta x$ is twice as strong as for $TbMn_2H_x$ in the same concentration range $1 \leq x \leq 4$. Both compounds have the same $C15$ structure with similar lattice parameters a and only slight differences in the hydrogen induced lattice expansion. At $T = 300$ K and $x \geq 1$ one has $\delta \ln a / \delta x \approx 1.8 \times 10^{-2}$ and 1.3×10^{-2} for $TbMn_2H_x$ (Ref. 14) and HfV_2H_x,[29] respectively. In $TbMn_2H_x$ the H atoms occupy the interstitial g sites (2Tb/2Mn) at all concentrations;[30] in HfV_2H_x there is a partial occupation of the interstitial e sites (3V/Hf) only at $x > 3$.

As will be discussed below, in the paramagnetic phase of $TbMn_2H_x$ the hydrogen atoms are moving rapidly among the g sites with residence times below 1 ns. The ^{111}Cd PAC time window is of the order of 500 ns. The frequency derived from the PAC spectra therefore corresponds to the time average of the QI. In Ref. 10 it has been shown that the g-site sublattice occupied by rapidly diffusing hydrogen can account only for a very minor part of the time-averaged QI. The observed concentration dependence of the EFG mainly reflects changes in the valence charge density close to the probe nucleus by the electrons provided by the hydrogen. The pronounced difference in the $\nu_q(x; T = 290$ K) dependence between HfV_2H_x and $TbMn_2H_x$ is therefore probably

related to differences in the band structure and in the H-induced redistribution of the electron states. For a detailed understanding of the resulting changes in the QI, first-principles calculations of the EFG at different H loads appear necessary.

Not only the concentration dependence $\nu_q(x;T=290\ \mathrm{K})$ of the static QI at room temperature but also its temperature variation $\nu_q(x=\mathrm{const};T)$ at a given hydrogen load x differ substantially between $R\mathrm{Mn_2H}_x$ and $\mathrm{HfV_2H}_x$. In $\mathrm{HfV_2H}_x$ the temperature coefficient $\alpha \equiv \delta \ln \nu_q / \delta T$ changes sign from $\alpha > 0$ at small x to $\alpha < 0$ at large x which has been related[10] to the hydrogen induced shift of the Fermi energy from a peak in the DOS to regions of small slowly varying DOS. Differently, hydrogenation of $R\mathrm{Mn_2}$ which shifts the Fermi energy to slightly larger DOS values[13] has very little effect on the temperature dependence of the ^{111}Cd QI (see Fig. 7). The temperature coefficient in $R\mathrm{Mn_2H}_x$ is negative at all hydrogen concentrations and up to $x \sim 3$ and $T > 350$ K practically the same as in uncharged $R\mathrm{Mn_2}$. Only at higher concentrations the temperature dependence increases; at $x \sim 4$ and $T \geq 400$ K where $R\mathrm{Mn_2H_4}$—rhombohedral at lower temperatures—has taken the $C15$ structure,[14] one finds $\alpha \sim -8(1) \times 10^{-4}\ \mathrm{K}^{-1}$ for hydrides and deuterides with R=Gd, Tb, and Dy which indicates a softening of the lattice possibly connected with the H induced lattice expansion.

C. Evidence for high H mobility in $R\mathrm{Mn_2H}_x$

While in the ^{111}Cd PAC spectra of $\mathrm{HfV_2H}_x$ the nuclear-spin relaxation caused by jumping H atoms is clearly visible (see Fig. 3), an attenuation of the periodic modulation of the anisotropy is not observed ($\lambda_2^{\max} \leq 0.5$ MHz) in the PAC spectra of $\mathrm{TbMn_2H}_x$ with the same $C15$ structure. In the Abragam-Pound limit[31] of fast dynamic perturbations with vanishing time average the relaxation parameter λ_2 depends on the fluctuation rate w and the strength of the fluctuating QI expressed by the frequency ν_q^f. For nuclear spin $I=5/2$ one has $\lambda_2 = 2.485(\nu_q^f)^2/w$. Both in $\mathrm{HfV_2H}_x$ and $\mathrm{TbMn_2H}_x$ with $x < 2$ the H atoms are randomly distributed on the 96g tetrahedral interstitial sites of the $C15$ structure.[30] In $\mathrm{TbMn_2H_{1.65}}$ ($a \sim 0.795$ nm), however, the distance of ^{111}Cd on Mn(V) sites to the nearest interstitial g site is about 10% larger than in $\mathrm{HfV_2H_{1.78}}$ ($a \sim 0.757$ nm). It can therefore be expected that in $\mathrm{TbMn_2H_{1.65}}$ the EFG produced at ^{111}Cd by an H ion on the nearest g site is smaller than in $\mathrm{HfV_2H_{1.78}}$. An estimate using a point-charge model of the EFG leads to a difference of $\sim 30\%$ in ν_q^f. The difference in the lattice parameters of $\mathrm{TbMn_2H_{1.65}}$ and $\mathrm{HfV_2H_{1.78}}$ could therefore explain a difference of a factor of 2 in the relaxation parameters but not the experimental factor ≥ 10. This leads us to conclude that the jump rate w in $\mathrm{TbMn_2H_{1.65}}$ must be much higher than in $\mathrm{HfV_2H_{1.78}}$ at the same temperature. The relaxation parameter $\lambda_2 \sim 6$ MHz at 300 K of the latter hydride corresponds[10] to a jump rate $w \sim 10^8\ \mathrm{s}^{-1}$. To explain the absence of spin-relaxation effects in $\mathrm{TbMn_2H}_x$ ($\lambda_2^{\max} \leq 0.5$ MHz) then it requires a jump rate of $w \geq 3 \times 10^9\ \mathrm{s}^{-1}$ at 300 K if the effect of the larger lattice parameter is included.

Quasielastic neutron-scattering (QENS) studies[32,33] provide evidence for two jump processes in $C15$-type hydrides: a fast localized motion within hexagons formed by g sites and a slower long-range H motion between hexagons. ^{111}Cd PAC measurements are probably sensitive only to the long-range jumps. The jump rate of the localized motion exceeds $10^{11}\ \mathrm{s}^{-1}$ at 300 K and the resulting relaxation would be too weak ($\lambda_2 \leq 5$ KHz) to be detected in the 500 ns time window of ^{111}Cd. In their QENS investigation of the H motion in $C15$ hydrides Skripov *et al.*[32,33] found that the jump rate of the long-range diffusional motion in $\mathrm{YMn_2H}_x$, $x \leq 1.2$, is at least 1 order of magnitude larger ($\mathrm{YMn_2H_{0.6}}$: $w = 7.7 \times 10^9\ \mathrm{s}^{-1}$ at 300 K) than in most other $C15$-type hydrides, which they relate to the geometry of the g-site sublattice characterized by the ratio r_2/r_1, where r_1 is the g-g distance within one hexagon and r_2 the g-g distance between nearest hexagons. While most $C15$-type hydrides have $r_2/r_1 > 1$, $\mathrm{YMn_2H}_x$, $x \leq 1.2$ is characterized by $r_2/r_1 = 0.78$ which doubles the number of jump directions for long-range diffusion for an H ion on a given g site. The same geometrical consideration may explain the high H mobility in $\mathrm{TbMn_2H}_x$ deduced from the ^{111}Cd PAC measurements; in $\mathrm{TbMn_2H_2}$ one has $r_2/r_1 = 0.70$ (with $a = 0.7955$ nm, $x = y = 0.42$, $z = 0.14$ from Ref. 27).

D. Information on structural and magnetic properties of $R\mathrm{Mn_2H}_x$

Although this investigation is mainly concerned with the influence of the H load on the QI in the $C15$ hydrides $R\mathrm{Mn_2H}_x$, the measurements also provide some information on the change in the structural and magnetic properties with the H content. One such topic is the two-step increase in the paramagnetic fraction of $\mathrm{TbMn_2H}_x$ for concentrations $x < 1.5$ (see Fig. 5). This observation is consistent with the structural and magnetic phase diagrams of $\mathrm{TbMn_2H}_x$ proposed by Figiel *et al.*[14] X-ray diffraction has provided evidence for spinodal decomposition at $x < 2$ and $T < 200$–250 K into a H-deficient cubic phase (α_o, $x \sim 0.05$, $T_N \sim 60$ K) and a H-rich cubic phase (α_r, $x \sim 1.7$, $T_N \sim 260$ K). The relative abundance of the H-deficient phase decreases with increasing x from $\sim 80\%$ at $x = 0.25$ to $< 20\%$ at $x = 1.5$. At $T > 200$ K, a single cubic phase (α_{im}; $T_N \sim 60$ K) precipitates at the expense of α_o and α_r.

For $x = 0.8$ the first increase in the paramagnetic fraction to $f_p \sim 0.5$ at 60–80 K reflects the transition of phase α_o to the paramagnetic state. $f_p \sim 0.5$ is in agreement with the relative abundance of phase α_o of $\sim 50\%$ reported in Ref. 14. Subsequently, f_p remains constant as long as the sample temperature is below the ordering temperature of phase α_r ($T_N \sim 260$ K). The precipitation of phase α_{im} at $T > 200$ K lowers the ordering temperature of the sample toward $T_N \sim 60$ K and results in the increase in f_p observed at $T > 200$ K. In the concentration range $1.5 \leq x \leq 1.7$ the abundance of phase α_o is below 20%. Therefore its magnetic transition is difficult to detect in the PAC spectra of $x = 1.65$. Up to $T \leq 250$ K one has $f_p \leq 0.1$ because $T < T_N$ of phase α_r. The subsequent increase in the $x = 1.65$ paramagnetic fraction to $f_p(300\ \mathrm{K}) \sim 1$ mirrors the increasing abundance

of phase α_{im} ($T_N \sim 60$ K). At $1.7 < x < 3.5$ there is only one cubic phase over the whole temperature range. Even so, our measurements indicate (see Fig. 5) that the transitions from the magnetically ordered to the paramagnetic phase—as in the case of phase α_o at $x=0.8$—extend over a finite temperature range of ~20–30 K suggesting a distribution of the ordering temperature. Such distributions—although usually narrower—have been found in most hyperfine spectroscopic studies of magnetically ordered intermetallic compounds.[34]

The concentration dependence of the ordering temperatures of $TbMn_2H_x$ derived from the PAC spectra agrees well with the results of Figiel *et al.*[14] and those of Przewoźnik *et al.*[22] for $DyMn_2H_x$ (see Fig. 6). The increase in the ordering temperature with increasing H load is correlated with the lattice expansion by H absorption and reflects the sensitivity of the Mn magnetic moment on the $d_{\text{Mn-Mn}}$ interatomic distance.[1]

V. SUMMARY

We have investigated the static and dynamic nuclear electric quadrupole interaction experienced by the nuclear probe $^{111}In/^{111}Cd$ on the Mn site of the $C15$ rare earth-manganese hydrides RMn_2H_x as a function of temperature and hydrogen content x. The trend of the Debye temperatures Θ_D of parent RMn_2 and corresponding RAl_2 derived from the temperature dependence of the ^{111}Cd QI is in agreement with the relation between Θ_D and the radius ratios r_R/r_{Mn} and r_R/r_{Al} postulated by Joseph and Gschneidner.[2,26] Both temperature and concentration dependence of the static QI of ^{111}Cd in RMn_2H_x differ substantially from the trends observed with the same probe in the isostructural hydrides HfV_2H_x. The measurements indicate that the H mobility in RMn_2H_x is at least 1 order of magnitude higher than in other Laves phase hydrides. The concentration dependence of the ordering temperature is in agreement with previous investigations.

*Corresponding author. forker@iskp.uni-bonn.de
†On leave from Physics Department, Panjab University, Chandigarh, India.

[1] V. Paul-Boncour, J. Alloys Compd. **367**, 185 (2004).
[2] K. A. Gschneidner, Jr. and V. K. Pecharsky, Z. Kristallogr. **221**, 375 (2006).
[3] A. A. Tulapurkar, V. V. Krishnamurthy, S. N. Mishra, and S. H. Devare, Hyperfine Interact. C1, 100 (1995).
[4] S. Demuynck, S. N. Mishra, A. A. Tulapurkar, S. Cottenier, J. Meersschaut, and M. Rots, Physica B (Amsterdam) **293**, 376 (2001).
[5] A. A. Tulapurkar and S. N. Mishra, Hyperfine Interact. **120-121**, 247 (1999).
[6] B. A. Komissarova, G. K. Ryasny, A. A. Sorokin, L. G. Shpinkova, A. V. Tsvyashchenko, and L. N. Fomichova, Phys. Status Solidi B **213**, 71 (1999).
[7] A. V. Skripov, M. Yu. Belyaev, and A. P. Stepanov, Solid State Commun. **71**, 321 (1989).
[8] D. T. Ding, J. I. de Lange, T. O. Klaassen, N. J. Poulis, D. Davidov and J. Shinar, Solid State Commun. **42**, 137 (1982).
[9] M. Peretz, J. Barak, D. Zamir, and J. Shinar, Phys. Rev. B **23**, 1031 (1981).
[10] M. Forker, W. Herz, D. Simon, and S. C. Bedi, Phys. Rev. B **51**, 15994 (1995), and references therein.
[11] M.-C. Huang, H. J. F. Jansen, and A. J. Freeman, Phys. Rev. B **37**, 3489 (1988).
[12] W. Däumer, H. R. Khan, and K. Lüders, Phys. Rev. B **38**, 4427 (1988).
[13] M. Pajda, R. Ahuja, B. Johansson, J. M. Wills, H. Figiel, A. Paja, and O. Eriksson, J. Phys.: Condens. Matter **8**, 3373 (1996).
[14] F. Figiel, A. Budziak, J. Żukrowski, G. Fischer, M. T. Keleman, and E. Dormann, J. Alloys Compd. **335**, 48 (2002).
[15] A. Weidinger, in *Topics in Applied Physics*, edited by L. Schlapbach (Springer, Berlin, 1992), Vol. 67.
[16] M. Forker, W. Herz, U. Hütten, M. Müller, R. Müßeler, J. Schmidberger, D. Simon, A. Weingarten, and S. C. Bedi, Nucl. Instrum. Methods Phys. Res. A **327**, 456 (1993).
[17] H. Frauenfelder and R. M. Steffen, in *Perturbed Angular Correlations*, edited by K. Karlsson, E. Matthias, and K. Siegbahn (North-Holland, Amsterdam, 1963).
[18] M. Blume, Phys. Rev. **174**, 351 (1968).
[19] H. Winkler and E. Gerdau, Z. Phys. **262**, 363 (1973).
[20] A. Baudry and P. Boyer, Hyperfine Interact. **35**, 803 (1987).
[21] M. Forker, W. Herz, and D. Simon, Nucl. Instrum. Methods Phys. Res. A **337**, 534 (1994).
[22] J. Przewoźnik, J. Żukrowski, K. Freindl, E. Japa, and K. Krop, J. Alloys Compd. **284**, 31 (1999).
[23] M. Forker and P. de la Presa, Phys. Rev. B **76**, 115111 (2007).
[24] D. Torumba, K. Parlinski, M. Rots, and S. Cottenier, Phys. Rev. B **74**, 144304 (2006).
[25] G. Schatz, E. Dafni, H. H. Bertschat, C. Bronde, F. D. Davidowski, and M. Haas, Z. Phys. B: Condens. Matter **49**, 23 (1982).
[26] R. R. Joseph and K. A. Gschneidner, Scr. Metall. **2**, 631 (1968).
[27] B. K. Vainshtein, V. M. Fridkin, and V. L. Indenbom, *Structure of Crystals*, 3rd ed. (Springer, Berlin, 1995).
[28] T. E. Scott, in *Handbook of Chemistry and Physics of Rare Earths*, edited by K. A. Gschneidner and L. Eyring (North-Holland, Amsterdam, 1978), Vol. 1.
[29] M. Yu. Belyaev, A. V. Skripov, A. P. Stepanov, M. E. Kost, and L. N. Paduretz, Sov. Phys. Solid State **28**, 1538 (1986).
[30] A. Budziak, F. Figiel, J. Żukrowski, E. Gratz, and B. Ouladdiaf, J. Phys.: Condens. Matter **13**, L871 (2001).
[31] A. Abragam and R. V. Pound, Phys. Rev. **92**, 943 (1953).
[32] A. V. Skripov, J. C. Cook, J. T. Udovic, M. A. Gonzalez, R. Hempelmann, and V. N. Kozhanov, J. Phys.: Condens. Matter **15**, 3555 (2003).
[33] A. V. Skripov, M. A. Gonzalez, and R. Hempelmann, J. Phys.: Condens. Matter **18**, 7249 (2006).
[34] M. Forker, S. Müller, P. de la Presa, and A. F. Pasquevich, Phys. Rev. B **68**, 014409 (2003).